27th ABCM International Congress of Mechanical Engineering
December 04-08, 2023, Florianópolis-SC, Brazil

COBEM-2023-0567
ANALYSIS OF THE TORSIONAL VIBRATION IN ROTODYNAMICS

Natália Rie Horikawa
natalia.horikawa@ufv.br
Paulo Cezar Büchner
paulo.buchner@ufv.br
Gladson Willian Pereira Rodrigues
gladson.rodrigues@ufv.br
Álisson Carlos Souza Rodrigues
alisson.rodrigues@ufv.br
Adiel Lima Pessôa
adiel.pessoa@ufv.br
Alexandre Martins Reis
amreis@ufv.br
Charles Luís da Silva
charles.silva@ufv.br
Geice Paula Villibor
geice.villibor@ufv.br
Universidade Federal de Viçosa. Av. PH Rolfs, s/n - Campus Universitário, Viçosa - MG, 36570-900

Abstract. *Rotodynamics is a branch of mechanical engineering that deals with the analysis and design of rotating machinery, such as pumps, turbines, and compressors. One of the main challenges in rotodynamic design is torsional vibration, which is a type of vibration that occurs when the twisting motion of a rotating shaft interacts with the stiffness and damping of the system. Torsional vibration can cause significant damage to the system, including fatigue failure, bearing damage, and couplings failure, leading to downtime and costly repairs. To mitigate this phenomenon, several techniques have been developed, including the use of damping devices, flexible couplings, and torsional vibration neutralizers. Torsional vibration is a complex phenomenon that can be difficult to measure accurately by indirect way. This type of vibration has a main challenge, which is the torsional vibration itself, which one occurs in rotational direction, and the vibration energy is typically transmitted through the shaft rather than the structure surrounding the system. In fact, the torsional vibrations waves have low intensity in lateral and axial directions, because of this, the sensors are not able to detect properly this phenomenon. The purpose of this work is to conduct a review of the fundamental principles of torsional vibration theory as the first step in the research effort. The comprehension of this phenomenon will permit subsequently explore potential solutions for the control of torsional vibration. On of this possibilities, for example, is the Micro Electro-Mechanical System technologies (MEMS). A prototype and a program routine in LabView/MatLab have implemented to analyze the acquired signal and manage the data, the results from this part of research will be presented in the next article.*
Keywords: *critical velocity, Holzer, Micro Electro-Mechanical, signal analysis.*

1. INTRODUCTION

The identification of torsional vibration effects in rotating machinery is of utmost importance for the development of rotodynamic projects, as this phenomenon is responsible for causing damages and premature failures in the structure. Torsional vibration is characterized by resulting oscillations in a rotating shaft due to the response of non-symmetric twisting forces (RAO, 2018) , where these forces are characterized by the presence of eccentricities, unbalances, or misalignment of the rotor.

The studies on this phenomenon date back to the early 20th century, where mathematical analyses allowed describing the behavior of torsional vibration in shafts, enabling understanding and evaluation of parameters related to the rotating system that influence the occurrence of this phenomenon. This knowledge evolution enabled the development of techniques to solve torsional vibration problems.

With the growth of the industrial sector, the use of rotating machines, such as compressors and turbines, has become more frequent, generating the need to know and work with torsional vibration measurement systems. In this context, Microelectromechanical Systems (MEMS) technologies stand out as an option to capture torsional vibration signals in practical applications. MEMS sensors are compact, wireless, and easy to implement, enabling real-time measurement of deformation present in the system when subjected to torsional vibration effects, as well as transmitting the signal to a signal analysis and control system.

The goal of this work is to explore current Microelectromechanical Systems (MEMS) technologies to solve the challenge of measuring torsional vibration in rotating machines. This approach includes creating a user-friendly prototype device adaptable to different machines, as well as developing a program using LabView/MatLab for the analysis of acquired signals and data management. Additionally, an experimental setup was constructed, comprising a rotor driven by a variable-speed motor and an embedded torsional excitation device. The integration of wireless sensors allows this setup to be part of the Internet of Things (IoT), a trend widely employed in the industry. The ultimate purpose of this research is to develop a torsional vibration control system in rotating machines through the implementation of wireless devices for detecting torsional vibration signals. This endeavor aims to contribute to the advancement of knowledge and application in this specific area of engineering.

2. TORSIONAL VIBRATION

Torsional vibrations in rotors occur due to the presence of angular oscillations along the axis of rotation, where the vibrational motion superimposes on the rotational motion of the shaft. Such vibrations are commonly predominant in power transmission systems where internal stresses can arise in the material due to oscillation, resulting in high cyclic loading that leads to shaft fatigue and ultimately component failure.

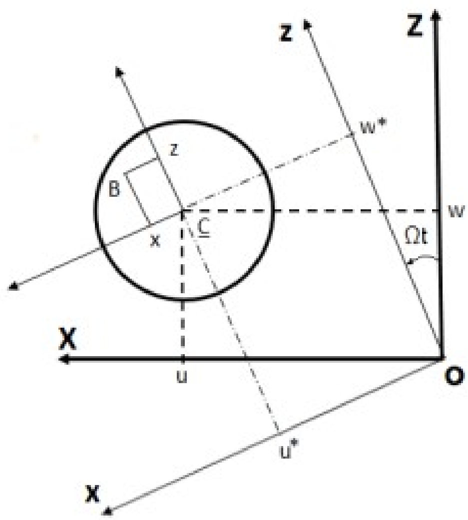

Figure 1. Coordinates of the geometric center C and an arbitrary point B on the shaft. (LALANNE and FERRARIS, 1996)

In rotating systems, the occurrence of lateral vibrations is also common. However, it is rare for lateral vibration to interact with torsional vibration, and the two vibrational phenomena can coincide without significant interaction. The equation governing the behavior of a rotating system consisting of an inertia disk coupled to a shaft and subjected to torsion with a degree of freedom is expressed as:

$$I_o\,\ddot{\theta} + C_t\,\dot{\theta} + K_t\,\theta = Mt(t), \tag{1}$$

M_t is the applied moment on the shaft, Io is the moment of inertia of the disk, Ct is the torsional damping coefficient, and kt is the torsional stiffness coefficient, which can be obtained using Eq. (2).

$$K_t = \frac{GJ}{l}, \tag{2}$$

G is the shear modulus of the material, J is the polar moment of area given by $J = \frac{\pi D^4}{32}$, and l is the length of the shaft subjected to torque.

Figure 2 represents a circular section shaft subjected to torsion, where the kinetic energy is given by eq. (3).

$$k = \frac{I_o\dot{\theta}^2}{2}, \tag{3}$$

$\dot{\theta}$ is the angular velocity of shaft rotation and I_o represents the mass moment of inertia, which is determined for an element of diameter D of the disk, expressed by eq. (4).

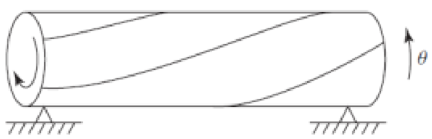

Figure 2. Shaft under torsion. (BÜCHNER, 2017)

$$I_o = \frac{\rho \pi D^4}{32} = \rho J. \tag{4}$$

Figure 3. Shaft element. (BÜCHNER, 2017)

Therefore, the kinetic energy per unit length of the element depicted in Figure 3 can be expressed as $I_o l$. Thus, the kinetic energy of an infinitesimal element at a node undergoing torsion can be obtained using eq. (5). (BÜCHNER, 2017).

$$K = \frac{\rho \pi R^4 l}{8}(\dot{\theta}_1^2 + \dot{\theta}_2^2), \tag{5}$$

the index accompanying the angular velocity $\dot{\theta}$ refers to which node the angular velocity is associated with. By eq. (5), it is possible to obtain the coefficient related to the mass matrix of the element, which is given by:

$$M = \frac{\rho \pi R^4 l}{4} \begin{bmatrix} 1 & 0 \\ 0 & 1 \end{bmatrix}. \tag{6}$$

To interpolate the torsion angles at the ends of the elements, eq. (6) is used, in which the linear relationship is given as a function of the position coordinate (y) and extends throughout the Y-axis.

$$\theta = \begin{bmatrix} 1 - \frac{y}{l} & \frac{y}{1} \end{bmatrix} \begin{bmatrix} \theta_1 \\ \theta_2 \end{bmatrix}, \tag{7}$$

the total kinetic energy in the torsional shaft is given by eq. (8).

$$K = \frac{1}{2} \int_l^0 I_\theta \dot{\theta}_2 dy, \tag{8}$$

substituting eq. (7) into the previous equation, the result is obtained by:

$$K = \frac{I_\theta l}{12} \left\{ \begin{smallmatrix} \dot{\theta_1} \\ \dot{\theta_2} \end{smallmatrix} \right\}^k \begin{bmatrix} 2 & 1 \\ 1 & 2 \end{bmatrix} \left\{ \begin{smallmatrix} \dot{\theta_1} \\ \dot{\theta_2} \end{smallmatrix} \right\}, \tag{9}$$

And the local mass matrix is:

$$M = \frac{I_\theta l}{6} \begin{bmatrix} 2 & 1 \\ 1 & 2 \end{bmatrix}. \tag{10}$$

Similarly, the elastic strain energy is given by eq.(11), where G is the shear modulus and J is the polar moment of inertia.

$$U = \frac{1}{2} \int_l^0 GJ \left(\frac{\partial \theta}{\partial y} \right)^2 dy, \tag{11}$$

for an infinitesimal element, the elastic strain energy is given by:

$$U = \frac{GJ}{2l}(\theta_1 - \theta_2)^2 = \frac{1}{2}k_t(\theta_1 - \theta_2)^2. \tag{12}$$

The stiffness constant is obtained from eq. (2). By substituting eq. (7) for the torsion angle (θ) into eq. (12), the equation for the elastic strain energy in matrix form is obtained, expressed as:

$$U = \frac{GJ}{l}\begin{Bmatrix}\theta_1\\\theta_2\end{Bmatrix}^K \begin{bmatrix}1 & -1\\-1 & 1\end{bmatrix}\begin{Bmatrix}\theta_1\\\theta_2\end{Bmatrix}, \tag{13}$$

thus, it is possible to obtain the local stiffness matrix described by:

$$K_t = \frac{GJ}{l}\begin{bmatrix}1 & -1\\-1 & 1\end{bmatrix}. \tag{14}$$

For a rotor, the global inertia matrix has a tri-diagonal format, which represents a combination of each local inertia matrix. Therefore, the stiffness matrix $[K]$, of size N, has the configuration:

$$[K] = \begin{bmatrix} K_1 - K_1 & & & \\ -K_1K_1 + K_2 - K_2 & & & \\ & -K_1K_i + K_{i+1} - K_{i\_1} & & \\ & & -K_{N-2}K_{N\_2} - K_{1N-1} \\ & & -K_{N-1}K_{N-1} \end{bmatrix} \tag{15}$$

K corresponds to the stiffness coefficient of the analyzed shaft.

3. MODELING OF THE ROTOR

Figure 4 depicts a representation of a rotor model, consisting of a shaft with a constant circular cross-section, the rotating element of the motor, an excitation disk, and an inertia disk.

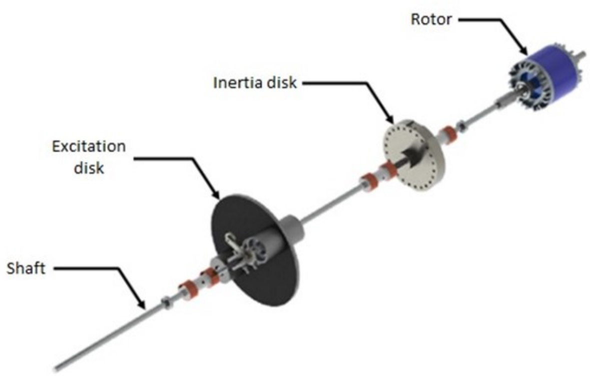

Figure 4. Rotor assembly. (BÜCHNER, 2017)

In this preliminary study, a modeling approach with concentrated masses was adopted, considering the inertias of the motor core, excitation disk, and inertia disk. Regarding the shaft, initially, only the torsional stiffness originating from that element was considered (BÜCHNER, 2017).

By analyzing the free-body diagram of the system, as illustrated in Figure 5, it was possible to derive the governing equations of this system using Newton's second law.

Thus, the set of governing equations of the system was obtained in matrix form, expressed by eq. (16).

$$M = \begin{bmatrix}I_m & 0 & 0\\0 & I_1 & 0\\0 & 0 & I_e\end{bmatrix}\begin{Bmatrix}\dddot{\theta}_m\\\ddot{\theta}_1\\\ddot{\theta}_e\end{Bmatrix} + \begin{bmatrix}k_{tm} & -k_{tm} & 0\\-k_{tm} & k_{tm}+k_{t1} & -k_{te}\\0 & -k_{te} & k_te\end{bmatrix}\begin{Bmatrix}\theta_m\\\theta_1\\\theta_e\end{Bmatrix} = \begin{Bmatrix}0\\0\\T_e\end{Bmatrix} \tag{16}$$

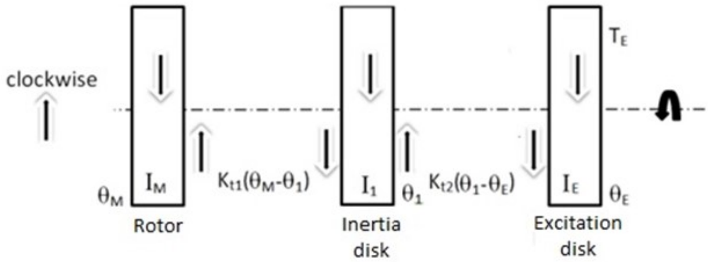

Figure 5. Free-body diagram - FBD. (BÜCHNER, 2017)

I_m, I_1, and I_e represent the inertias of the rotor, inertia disk, and excitation disk, respectively. k_{t1} and k_{t2} are the stiffness constants corresponding to segments 1 and 2, and θ_m, θ_1, and θ_e represent the angular variations of each inertia component.

It is important to note that this analysis is conducted on a primary system that is undamped, linear, and time-invariant (BÜCHNER, 2017).

To obtain the natural vibration frequencies of the system, a programming sequence was developed using MatLab software, where the natural frequencies were calculated through the eigenvalue problem resolution method and the Holzer method, which proposes to estimate the torsional natural frequencies by assuming a frequency and unitary amplitude at one end of the system, allowing the calculation of all other deflections in the system. (J.QUIROGA, 2019). The results are presented in Table 1, where it is registered the 0 Hz which is referred to as rigid body vibration, and the others are the tow natural frequencies. Thus, the first one correspond the rigid body vibration, 53 and 190 Hz are the next two normal modes of torsional vibration (BÜCHNER, 2017).

Table 1. Undamped Natural Frequencies. The first frequency at 0 Hz is referred to as rigid body vibration, and the others are the two natural frequencies.

i	Matlab	Holzer
Ω_0	0 Hz	0 Hz
Ω_1	53 Hz	53 Hz
Ω_2	190 Hz	190 Hz

Author's source.

The result obtained through the Holzer's method is presented in Figure 6. Due to the magnitude of the amplitudes, the graph has been divided into two parts. To facilitate visualization, an alternative representation of this graph is shown in Figure 7.

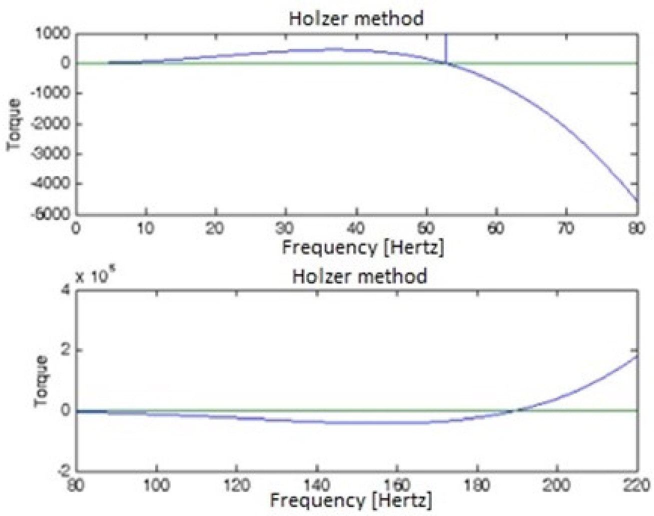

Figure 6. Holzer's method.

As it can be noted, in this scale, all the natural torsional frequencies are clearly observed into the range selected.

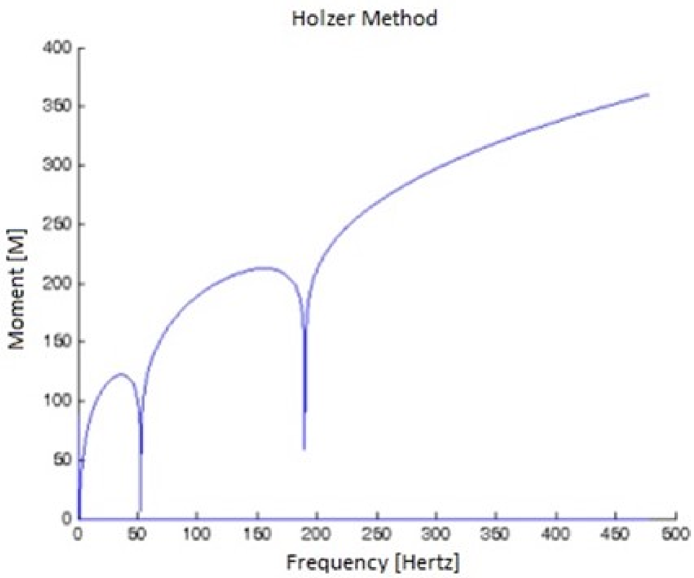

Figure 7. Hozer's method using a logarithmic scale as proposed by (BÜCHNER, 2017)

The critical speeds of the system can be examined using the Campbell Diagram, as shown in Figure 8, where the torsional natural frequencies (identified on the vertical axis) are plotted against the rotation of the excitation system (identified on the horizontal axis). The critical torsional speed is determined by the intersection of the inclined line with the lines representing the natural frequencies (LALANNE and FERRARIS, 1996).

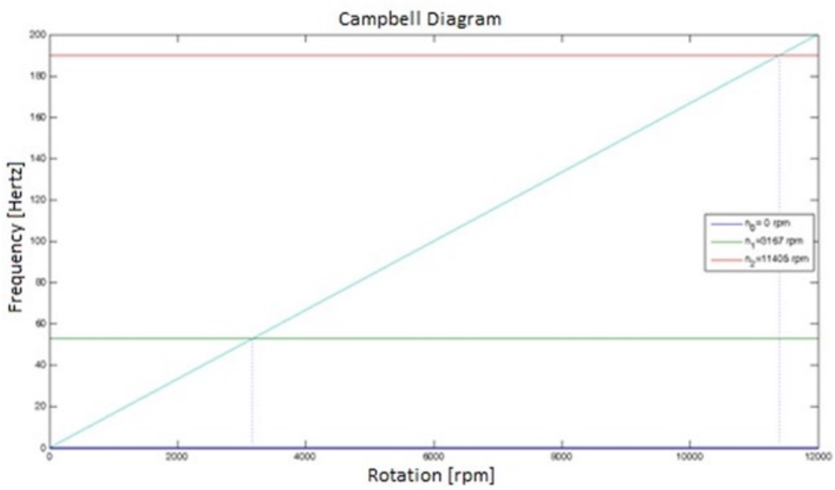

Figure 8. Campbell diagram of the system.

4. CONCLUSION

In conclusion, this preliminary study adopted a linear modeling approach to analyze the torsional vibration of a rotor system. The governing equations of the system were derived by Newton's second law. The analysis was conducted on an undamped, linear, and time-invariant primary system.

To determine the natural vibration frequencies, a programming sequence was created using MATLAB. Holzer's solution method were employed to calculate the natural frequencies of the system, which are summarized in Table 1. An effective approach for presenting Holzer's graphs to identify the natural frequencies was also introduced.

The critical torsional speed of the system was examined using the Campbell Diagram in Figure 8, where torsional natural frequencies were plotted against the rotation of the excitation system. The critical torsional speed was determined by the intersection of the inclined line with the lines representing the natural frequencies.

This initial study has provided valuable insights into the behavior of the rotor system and its torsional natural frequencies, which are essential for understanding this phenomenon in rotodynamics.

5. REFERENCES

BÜCHNER, P.C., 2017. *Modelagem de neutralizador dinâmico de vibrações torcionais viscoelástico aplicado em sistemas rotodinâmicos*. Ph.D. thesis, Graduate Program in Mechanical Engineering, COPPE - Federal University of Rio de Janeiro, Rio de Janeiro, Brasil.

J.QUIROGA, e.a., 2019. "Torsional natural frequencies by holzer method". *Journal of Physics: conferece Series*, Vol. 1160, p. 012008.

LALANNE, M. and FERRARIS, G., 1996. *Rotodynamics Prediction in engineering 2a. ed.* Editora Orsa Maggiore, Florianópolis.

RAO, S.S., 2018. *Mechanical vibration 6th ed.* United Kingdom.

6. RESPONSIBILITY NOTICE

The authors are solely responsible for the printed material included in this paper.